Published in final edited form as:
Mol Cell. 2011 November 18; 44(4): 517–531. doi:10.1016/j.molcel.2011.10.001.

A unified model of mammalian BCL-2 protein family interactions at the mitochondria

Fabien Llambi[1], **Tudor Moldoveanu**[1], **Stephen W.G. Tait**[1], **Lisa Bouchier-Hayes**[1,3,4], **Jamshid Temirov**[2], **Laura L. McCormick**[1], **Christopher P. Dillon**[1], and **Douglas R. Green**[1,*]

[1]Department of Immunology, St. Jude Children's Research Hospital, 262 Danny Thomas Place, Memphis, TN38105, U.S.A

[2]Cell and Tissue Imaging, St. Jude Children's Research Hospital, 262 Danny Thomas Place, Memphis, TN38105, U.S.A

[3]Center for Cell and Gene Therapy, Baylor College of Medicine, Houston, Texas, USA

[4]Department of Pediatrics-Hematology, Baylor College of Medicine, Houston, Texas, USA

Summary

During apoptosis, the BCL-2 protein family controls Mitochondrial Outer Membrane Permeabilization (MOMP), but the dynamics of this regulation remains controversial. We employed chimeric proteins composed of exogenous BH3 domains inserted into a tBID backbone that can activate the pro-apoptotic effectors BAX and BAK to permeabilize membranes without being universally sequestered by all anti-apoptotic BCL-2 proteins. We thus identified two "modes" whereby pro-survival BCL-2 proteins can block MOMP, by sequestering direct activator BH3-only proteins ("MODE 1") or by binding active BAX and BAK ("MODE 2"). Notably, we found that MODE 1 sequestration is less efficient and more easily de-repressed to promote MOMP than MODE 2. Further, MODE 2 sequestration prevents mitochondrial fusion. We provide a unified model of BCL-2 family function that helps to explain otherwise paradoxical observations relating to MOMP, apoptosis, and mitochondrial dynamics.

Introduction

The BCL-2 protein family regulates the intrinsic apoptotic pathway by controlling the mitochondrial outer membrane integrity (Llambi and Green, 2011). Additionally, the BCL-2 family modulates the balance between mitochondrial fission and fusion (Martinou and Youle, 2011), and is thereby linked to mitochondrial physiology.

BCL-2 proteins can be categorized into multidomain proteins, that share a similar globular structure with four BCL-2 homology regions (BH1, BH2, BH3 and BH4), and BH3-only proteins, which contain only one BH region (BH3). BH3-only proteins (e.g. BID, BIM, PUMA, BAD, NOXA) are pro-apoptotic whereas multidomain BCL-2 proteins can be either anti-apoptotic (e.g. BCL-2, BCL-w, BCL-xL, MCL-1 and BFL1/A1) or pro-apoptotic (e.g. BAX and BAK). BAX and BAK are the effectors of the BCL-2 family as upon activation,

*Correspondence: douglas.green@stjude.org.

they change conformation, insert into the outer mitochondrial membrane, oligomerize and induce mitochondrial outer membrane permeabilization (MOMP) (Chipuk et al., 2010).

Pro- and anti-apoptotic members of the BCL-2 family antagonize each other through protein-protein interactions. Indeed, structural analysis of pro-survival BCL-2 family members reveals a characteristic hydrophobic pocket that acts as a receptor for the BH3 domain of effector or BH3-only proteins allowing their sequestration and MOMP inhibition (Petros et al., 2004). This hydrophobic groove can be pharmacologically targeted by small molecule inhibitors, such as ABT-737, that mimic the action of a BH3-domain (Oltersdorf et al., 2005).

Several models have been proposed to explain how BCL-2 proteins regulate outer mitochondrial membrane integrity. The “neutralization model” (Uren et al., 2007; Willis et al., 2005; Willis et al., 2007) stipulates that BAX and BAK activation is a spontaneous event and consequently, neutralization of the full repertoire of anti-apoptotic BCL-2 proteins by BH3-only proteins is sufficient to induce BAX and BAK oligomerization and MOMP. The “direct activation model” (Kuwana et al., 2005; Kuwana et al., 2002; Letai et al., 2002; Wei et al., 2000) posits that BH3-only proteins are divided into “de-repressors/sensitizers”, whose sole function is to bind and inhibit anti-apoptotic proteins (e.g., BAD), and “direct-activators” (e.g. BID, BIM) that can also transiently interact with and activate the effectors BAX and BAK. Finally the “embedded together” model proposes that anti-apoptotic proteins act as dominant negative regulators of BAX and BAK by binding to direct activators and effectors in membranes, inhibiting both the activation and the oligomerization step (Leber et al., 2007; Leber et al., 2010).

In this study we define a unified model compatible with and incorporating components of each model, integrating the fundamental features of BCL-2 protein interactions inherent to the regulation of the outer mitochondrial membrane integrity and mitochondrial dynamics. We define two “modes” in which anti-apoptotic proteins prevent apoptosis: by sequestering direct activators of the effectors (MODE 1) or the activated effectors themselves (MODE 2). By probing conditions favoring one mode of sequestration or another, we reveal general properties of BCL-2 protein function that account for apparently paradoxical phenomena that are not readily explained by other models.

Results

Chimeric direct activators of BAX and BAK

Elucidating how BCL-2 proteins regulate MOMP is complicated since direct activator BH3-only proteins (e.g. BID, BIM, and perhaps PUMA) are universally sequestered by anti-apoptotic BCL-2 proteins ((Certo et al., 2006; Chen et al., 2005; Kuwana et al., 2005). Consequently, the pro-apoptotic function of a direct activator can be attributed to either the activation of BAX and BAK, or to the inhibition of the full repertoire of pro-survival BCL-2 family members. To circumvent this, we designed direct activator proteins with a more restricted binding pattern. Upon activation, BAX and BAK change conformation and expose their BH3 domain (Dewson et al., 2008; Gavathiotis et al., 2010; Kim et al., 2009), thus inducing a “feed-forward” mechanism to activate other native molecules of BAX (and probably BAK) (Gavathiotis et al., 2010). In contrast to BID and BIM however, BAX and BAK do not bind all anti-apoptotic proteins with the same affinity (Willis et al., 2005; Zhai et al., 2008). Since replacement of the BIM BH3 domain by that of another BH3-only protein changes its binding spectrum and activity (Mérino et al., 2009), we reasoned that a similar strategy might be applied to the BID BH3 domain, replacing it with those of multidomain BCL-2 proteins such as BAX and BAK to create new specific direct activators.

To test this, the BH3 domains of BIM, BCL-2, BCL-w, BCL-xL, MCL-1, BAX and BAK were cloned into the active BID C-terminal fragment (tBID) (Figure 1A). To control whether substitution of tBID BH3 domain interferes with its sub-cellular localization, GFP-tBID and GFP-tBID^{BH3} chimeric proteins were co-expressed with mito-dsRed in HeLa cells and examined by confocal microscopy. All of the chimeras displayed appropriate mitochondrial localization (Figure 1B). Next, HeLa cells were transiently transfected with expression constructs for wild type and tBID^{BH3} chimeric proteins and cell death was measured by Annexin V staining and flow cytometry analysis. The BH3 domains of BIM, BAX and BAK reconstituted tBID pro-apoptotic activity, whereas the BH3 domains from the anti-apoptotic proteins BCL-2, BCL-w, BCL-xL and MCL-1 did not (Figure 1C). Accordingly, HeLa cells expressing the mitochondrial inter-membrane space marker Omi-mCherry underwent MOMP when tBID, tBID$^{BIM-BH3}$, tBID$^{BAX-BH3}$ and tBID$^{BAK-BH3}$ were expressed (Figure 1D and Figure S1).

To examine the specific activity of the tBID chimeric proteins on BAX or BAK, mitochondria-enriched heavy membrane (MHM) fractions were purified from WT or *bak*$^{-/-}$ mouse livers which display BAK but not BAX or neither effector respectively (Hsu et al., 1997). The tBID chimeric proteins were added to *bak*$^{-/-}$ MHM together with recombinant full-length BAX or to WT MHM (Figure 1E and 1F respectively) and MOMP was assessed by monitoring cytochrome *c* release. In the presence of BAX or BAK, tBID$^{BIM-BH3}$, tBID$^{BAX-BH3}$, and tBID$^{BAK-BH3}$ displayed activity similar to tBID, while tBID$^{BCL-2-BH3}$, tBID$^{BCL-w-BH3}$, tBID$^{BCL-xL-BH3}$ and tBID$^{MCL-1-BH3}$ did not (Figures 1E and 1F). To determine if tBID$^{BIM-BH3}$, tBID$^{BAX-BH3}$ and tBID$^{BAK-BH3}$ directly activate the effectors, we tested their ability to induce membrane permeabilization of large unilamelar vesicles (LUV) by recombinant BAX or BAK-ΔC (Figure 1F and 1G respectively). As previously described (Kuwana et al., 2002), incubation of LUV with recombinant BAX or BAK-ΔC effectively released fluorescent dextran when tBID was present. Notably, tBID$^{BIM-BH3}$, tBID$^{BAX-BH3}$ and tBID$^{BAK-BH3}$ activated BAX or BAK to permeabilize LUV to the same extent as wild type tBID. Collectively, these results indicate that all of the tBID^{BH3} chimeras localize to the mitochondria, yet only the BH3 domains of BIM, BAX or BAK reconstitute tBID pro-apoptotic activity and directly activate the effectors BAX and BAK to induce MOMP.

Anti-apoptotic BCL-2 proteins inhibit MOMP through two distinct mechanisms

Since the BH3 domain of pro-apoptotic BCL-2 proteins dictates the binding specificity to the anti-apoptotic proteins (Certo et al., 2006; Chen et al., 2005), we assessed whether tBID^{BH3} chimeras display a binding pattern similar to that of the full-length proteins from which they were derived. FLAG-tagged full length BIM-s, BAX, BAK, tBID and tBID^{BH3} chimeras (Figure 2A and 2B) were co-expressed with HA-tagged BCL-2, BCL-xL or MCL-1 in 293T cells. FLAG-tagged proteins were immunoprecipitated with anti-FLAG antibody in the presence of 0.5% NP40 (which promotes BAX and BAK activation (Hsu and Youle, 1997)), and were examined for anti-apoptotic BCL-2 protein binding by HA immunoblot. All tBID^{BH3} chimeras faithfully mirrored the interaction profile of their full-length relative: BAX and tBID$^{BAX-BH3}$ displayed preference for binding BCL-2 and BCL-xL over MCL-1, whereas BAK and tBID$^{BAK-BH3}$ interacted more strongly with BCL-xL and MCL-1, but only poorly with BCL-2. BIM and tBID$^{BIM-BH3}$ displayed similar binding to the three anti-apoptotic proteins (Figures 2A and 2B). Remarkably, the replacement of the tBID BH3-domain with that of BAX or BAK sustains the direct activator function of tBID but changes its binding profile (Figure 2C).

Based on the specificities of the anti-apoptotic proteins for BAX/tBID$^{BAX-BH3}$ and BAK/tBID$^{BAK-BH3}$, we envisioned four scenarios whereby anti-apoptotic and pro-apoptotic BCL-2 proteins can interact (Figure 2D): The anti-apoptotic protein can bind (a) both direct

activator and effector (orange box), (b) the direct activator but not the effector (which we call MODE 1 sequestration, red box), (c) the effector but not the direct activator (MODE 2 sequestration, purple box), or (d) neither (blue box). We generated conditions for each scenario by incubating tBID, $tBID^{BIM\text{-}BH3}$, $tBID^{BAX\text{-}BH3}$, or $tBID^{BAK\text{-}BH3}$ with either *bak*$^{-/-}$ MHM in the presence of recombinant BAX (Figure 2E) or with WT MHM (expressing BAK) (Figure 2F) and BCL-2-ΔC, BCL-xL-ΔC or MCL-1-ΔC. MOMP did not ensue when the anti-apoptotic proteins were capable of inhibiting both direct activator and effector (e.g. tBID-WT+BAX+BCL-xL, or tBID-WT+BAK+BCL-xL; orange boxes). Interestingly, MODE 1 inhibition of the direct activator alone (e.g. $tBID^{BAK\text{-}BH3}$+MCL-1+BAX, or $tBID^{BAX\text{-}BH3}$+BCL-2+BAK; red boxes) and MODE 2 inhibition of the effector alone (e.g. $tBID^{BAK\text{-}BH3}$+BCL-2+BAX, or $tBID^{BAX\text{-}BH3}$+MCL-1+BAK; purple boxes) were each sufficient to inhibit MOMP. In contrast, MOMP occurred when the anti-apoptotic protein was unable to bind to the direct activator and the effector (e.g. $tBID^{BAX\text{-}BH3}$+MCL-1+BAX, or $tBID^{BAK\text{-}BH3}$+BCL-2+BAK, blue boxes). Therefore, anti-apoptotic BCL-2 proteins inhibit MOMP either by sequestering the direct activator BH3-only proteins or the activated effectors, BAX and BAK.

Protease sensitivity reports BAK activation status

We sought a method to discriminate between the two modes of inhibition of MOMP in cells. Following activation, BAK partially unfolds and exposes its N-terminal and BH3 regions (Dewson et al., 2008; Kim et al., 2009). We reasoned that these conformational changes might be detected through limited proteolysis by calpain, a protease that has poorly defined substrate specificity rather cleaving unstructured regions based on accessibility (Friedrich and Bozóky, 2005). Thus, FLAG-tagged BAK was immunoprecipitated from 293T cells in the presence of CHAPS or NP40 and subjected to limited calpain proteolysis (Figure 3A). Previous work has shown that the non-ionic detergent NP40 activates BAK independently of apoptotic stimulation whereas the zwitterionic detergent CHAPS does not (Hsu and Youle, 1997). Accordingly, proteolysis of BAK was not observed in the presence of CHAPS whereas two cleaved fragments were detected in the presence of NP40 (Figure 3A). Strikingly, the appearance of one of the cleavage products was reduced upon co-transfection with BCL-xL and MCL-1 (which bind BAK in non-ionic detergents) but not with BCL-2 (which does not) (Willis et al., 2005), suggesting that calpain differentially cleaves active and sequestered BAK. The calpain cleavage sites in activated human BAK (BAK1) were identified by mass spectrometry (Figure S2A). These were mapped to Arg42-His43 at the end of the BH4 domain (hereafter referred to as “BH4 cleavage”) (Kvansakul et al., 2008)) and Arg87-Arg88 within the BH3 domain (“BH3 cleavage”) (Figure 3B and Figure S2A). Therefore, limited calpain proteolysis of BAK detects previously described features of BAK activation, i.e. exposure of the N-terminal BH4 region and BH3 domain (Dewson et al., 2008; Kim et al., 2009).

We then tested whether calpain differentially cleaves inactive and active BAK on purified mitochondria. WT MHM were incubated with tBID, BIM-s, BAD or NOXA and treated with recombinant calpain (Figure 3C). Inactive BAK (i.e. on untreated mitochondria or treated with de-repressor BH3-only proteins BAD or NOXA (Kim et al., 2006; Kuwana et al., 2005; Letai et al., 2002)) was not cleaved by calpain, whereas activated BAK (i.e. treated with the direct activators tBID or BIM-s (Kim et al., 2006; Kuwana et al., 2005; Letai et al., 2002)) became sensitive to calpain proteolysis at both sites (BH4 and BH3), producing two cleaved fragments. Tellingly, BAK sensitivity to calpain correlated with MOMP (Figure 3C lower panel), further underscoring the correlation between calpain cleavage of BAK and activation status.

We next examined BAK cleavage pattern in apoptotic cells. HeLa cells were induced with UV irradiation, actinomycin D or staurosporine in the presence of the pan-caspase inhibitor Q-VD-OPH to preserve cell integrity upon apoptosis induction. After 12 hr, cells were digitonin permeabilized and incubated with recombinant calpain (Figure S2B, upper panel). Alternatively, we assessed apoptosis by excluding caspase inhibitor and digitonin (Figure S2B, lower panel). The two cleaved products of BAK were strictly produced in apoptotic cells, indicating that unstimulated cells present BAK inactive/dormant conformations. Thus, to drive apoptosis, activated BAK achieves conformation accessible to exogenous calpain proteolysis.

We then interrogated whether binding to an anti-apoptotic protein alters the digestion profile of native BAK. WT MHM were incubated with tBID in the presence or absence of low concentrations of BCL-xL-ΔC (50 nM) and subjected to limited calpain proteolysis (Figure 3D, upper panel). Cytochrome *c* release was blocked when BCL-xL-ΔC was present (Figure 3D, lower panel), yet BAK was sensitive to partial calpain proteolysis, generating one stable fragment (BH4 cleavage). A similar digestion profile was obtained from UV treated BCL-xL over-expressing HeLa cells which resist apoptosis (Figure S2C). Together, these results suggest that the BH3 domain is inaccessible to calpain proteolysis when active BAK is sequestered, consistent with previous work showing that, to mediate interaction, the BAK BH3 domain is buried in the hydrophobic groove of anti-apoptotic BCL-2 proteins (Sattler et al., 1997).

We further interrogated BAK activation status in MODE 1 vs. MODE 2 sequestration. tBID, $tBID^{BIM\text{-}BH3}$, $tBID^{BAX\text{-}BH3}$, $tBID^{BAK\text{-}BH3}$ were incubated with WT MHM in the presence of high concentrations (1μM) of BCL-2-ΔC, BCL-xL-ΔC or MCL-1-ΔC in order to more exclusively engage one of the two inhibition modes (as in Figure 2F) and the MHM were subjected to calpain digestion (Figure 3E). As expected, addition of $tBID^{BIM\text{-}BH3}$, $tBID^{BAX\text{-}BH3}$ or $tBID^{BAK\text{-}BH3}$ to mitochondria produced both cleavage products of BAK, similarly to tBID (Figure 3E, upper panel). In contrast, anti-apoptotic proteins able to bind the direct activator (orange and red boxes) precluded calpain cleavage of BAK, consistent with the idea that in MODE 1 repression, direct activators are fully sequestered by anti-apoptotic proteins and BAK is not activated. However, when the anti-apoptotic proteins strictly sequestered BAK (MODE 2, purple box), BAK BH4 cleavage was observed. Finally, is presence of anti-apoptotic proteins unable to bind either direct activator or effector, BAK was cleaved at both the BH4 and BH3 cleavage sites (blue box). Therefore, in MODE 1 repression (sequestration of the direct activator) BAK remains inactive while in MODE 2 repression, BAK is activated and sequestered by anti-apoptotic BCL-2 proteins (Figure 3E).

Inhibition of MOMP by MODE 1 is less efficient than that of MODE 2

We next sought to evaluate the relative efficiencies of both modes of repression to inhibit MOMP by incubating $tBID^{BAX\text{-}BH3}$ or $tBID^{BAK\text{-}BH3}$ with WT or $bak^{-/-}$ MHM (supplemented with recombinant BAX) in the presence of a range of concentrations of recombinant BCL-2 or MCL-1 (Figure 4A). We found that inhibition of MOMP via MODE 1 ($tBID^{BAK\text{-}BH3}$+MCL-1+BAX or $tBID^{BAX\text{-}BH3}$+BCL-2+BAK) required significantly more anti-apoptotic protein than via MODE 2 ($tBID^{BAK\text{-}BH3}$+BCL-2+BAX, or $tBID^{BAX\text{-}BH3}$+MCL-1+BAK) suggesting that anti-apoptotic proteins acting in MODE 2 are more efficient than those in MODE 1.

Based on this finding, we reasoned that MODE 1 complexes should be more readily de-repressed to cause MOMP than those in MODE 2. To test this, WT MHM (containing BAK) were incubated with $tBID^{BAX\text{-}BH3}$ plus BCL-2 (MODE 1) or $tBID^{BAX\text{-}BH3}$ plus MCL-1 (MODE 2). After one hour, “de-repressor” BH3 peptides from BAD or NOXA were added

and cytochrome *c* release was assessed (Figure 4B). The BAD-BH3 binds specifically to BCL-2 and NOXA-BH3 to MCL-1 with comparable affinities for their respective anti-apoptotic protein (Certo et al., 2006; Chen et al., 2005). MODE 1 inhibition of the direct activator could be overcome by a low concentration of de-repressor peptide ($tBID^{BAX\text{-}BH3}$+BAK+BCL-2+BAD, red box) but a higher concentration was necessary to induce MOMP during MODE 2 effector engagement ($tBID^{BAX\text{-}BH3}$+BAK +MCL-1+NOXA, purple box). Therefore, both are competent to inhibit MOMP, but MODE 1 is less efficient than MODE 2 sequestration, and more readily de-repressed to cause MOMP. This observation cannot be accounted for simply by a difference in BH3 domain affinity for anti-apoptotic proteins, suggesting that the interaction between the anti-apoptotic and effector proteins may extend beyond the canonical BH3:hydrophobic groove. This is consistent with recent observations that the interaction of BAX with BCL-2 and BCL-xL includes additional interactions outside the BH3 domain of BAX and may also involve an additional interface at the “back” of both molecules (α-1/α-6 helices) (Ding et al., 2010; Ku et al., 2011).

BCL-xL blocks MOMP sequentially through MODE 1 and MODE 2

Next, we sought to investigate the dynamics underlying MOMP inhibition when the anti-apoptotic protein can inhibit both direct activator and effector proteins. WT MHM were incubated with a range of concentrations of recombinant cleaved BID (n/c BID) in the presence or absence of 100 nM recombinant full-length BCL-xL. MHM were then treated with calpain or analyzed for cytochrome *c* release (Figure 5A). All concentrations of n/c BID (1 nM to 1 μM) induced full BAK activation (BH3 and BH4 cleavage) and MOMP in the absence of BCL-xL (Figure 5A, left panel). BCL-xL efficiently inhibited cytochrome *c* release and BAK activation at low concentrations of n/c BID (1 and 10 nM) consistent with MODE 1 inhibition (Figure 5A, right panel). Interestingly, an equimolar concentration of n/c BID and BCL-xL (100 nM) induced BAK BH4 cleavage by calpain in the absence of MOMP, consistent with MODE 2 inhibition. Finally, excess n/c BID (1 μM) induced full BAK activation and MOMP. We recapitulated similar dynamics in HeLa cells expressing a range of tBID concentrations (Figure 5B). Over-expression of BCL-xL completely inhibited BAK activation and calpain cleavage induced by low tBID expression (50 ng). Under these conditions, tBID was sequestered by BCL-xL in MODE 1 (Figure S3). Higher tBID expression (500 ng of plasmid) consistently promoted the appearance of the sequestered form of BAK (MODE 2 inhibition).

HeLa cells stably over-expressing BCL-xL or an empty vector were next exposed to UV irradiation and subjected to calpain digestion (Figure 5C, upper panel), monitored for cytochrome *c* release (Figure 5C, middle panel) or quantified for cell death (Figure 5C, lower panel). Under these conditions, low UV exposures were able to induce BAK activation, MOMP, and cell death in control cells while having little effect on BAK activation in BCL-xL over-expressing cells. Only higher UV irradiation was able to induce BAK activation (BH4 cleavage) in the absence of MOMP and cell death in the BCL-xL over-expressing cells. These results suggest that increasing concentrations of direct activator sequentially induce MODE 1 and then MODE 2 inhibition by anti-apoptotic BCL-2 proteins.

We further reasoned that since MODE 1 sequestration is more easily de-repressed than MODE 2 sequestration, a sub-lethal concentration of de-repressor should induce a transition from MODE 1 to MODE 2. To test this, a range of concentrations of BAD-BH3 peptide or ABT-737 was added subsequent to WT MHM incubation with 10 nM n/cBID and 100 nM full-length BCL-xL, (Figure 5D). Consistent with Figure 5A, this tBID/BCL-xL ratio did not induce BAK activation (as detected by calpain cleavage), suggesting that only MODE 1 complexes (tBID:BCL-xL) were present (Figure 5A). However, the addition of 2 μM BAD-

BH3 peptide or ABT-737 induced BAK activation without MOMP, suggesting that, at this concentration, BAD-BH3 and ABT-737 displace tBID from BCL-xL without impairing the ability of BCL-xL to inhibit activated BAK. As expected, higher concentrations of BAD-BH3 or ABT-737 were able to fully de-repress both modes of sequestration and induced full BAK activation as well as MOMP. Thus, sub-lethal de-repression can convert MODE 1 into MODE 2.

In the presence of BCL-xL, activated BAX translocates to the mitochondria without inducing MOMP

In contrast to BAK, "inactive/dormant" BAX is cytosolic in healthy cells and translocates to mitochondria upon activation (Hsu et al., 1997). We speculated that MODE 2 sequestration of BAX would be observed as mitochondrial translocation without MOMP induction. HeLa cells stably expressing Omi-mCherry and Venus-BAX in the presence or absence of over-expressed BCL-xL were subjected to UV irradiation and imaged by live cell microscopy (Figure 6A and Movies S1 and S2). We observed that BAX translocated to mitochondria almost simultaneously with MOMP in control cells. However, in cells over-expressing BCL-xL, a gradual accumulation of Venus-BAX at the mitochondria was observed without evidence of MOMP. BAX translocation was quantified by spatial correlation (Pearson's correlation coefficient (Adler and Parmryd, 2010)) between Omi-mCherry and Venus-BAX (Figure 6B). Strikingly, there was a significant delay between the onset of BAX translocation and MOMP in control HeLa cells (4 to 6 hr) and BAX translocation in the absence of MOMP in BCL-xL over-expressing cells (10 to 12 hr). This suggests that in the presence of BCL-xL, BAX translocation to the mitochondria without MOMP only occurs in response to higher levels of direct activator proteins that accumulate over time, consistent with MODE 2 inhibition.

To test this hypothesis, we quantified Venus-BAX translocation in response to increasing levels of stress. HeLa cells stably expressing Omi-mCherry and Venus-BAX in the presence or absence of over-expressed BCL-xL were subjected to a range of UV in the presence of Q-VD-OPH, permeabilized after 30h with digitonin to remove cytosolic proteins and assessed by flow cytometry (Figures 6C and 6D). Control HeLa cells simultaneously showed a loss of Omi-mCherry (as a marker for MOMP) and a gain of Venus-BAX (as a marker for BAX translocation to the mitochondria). However, cells over-expressing BCL-xL displayed an accumulation of Venus-BAX correlated to the intensity of UV treatment without loss of the mCherry signal, thus suggesting that in the presence of anti-apoptotic proteins and upon apoptotic signaling, BAX is activated and sequestered (MODE 2) at the mitochondria without inducing MOMP.

We further tested if BAX sequestered in MODE 2 could be detected by BAX-6A7 antibody, which specifically recognizes a conformational change in the N-terminal region of active BAX (Hsu et al., 1997). While BAX translocated to the mitochondria in response to UV irradiation in both HeLa and HeLa-BCL-xL cells (Figure S4B), BAX was only immunoprecipitated by the 6A7 antibody in the former (Figure S4A). This indicates that the 6A7 epitope is not accessible in active BAX sequestered in MODE 2, consistent with a previous report that BAX complexed with BCL-xL in non-ionic detergent is not recognized by BAX-6A7 antibody (Hsu and Youle, 1997).

To test if sequestered BAX is inserted or loosely associated with the outer mitochondrial membrane, HeLa cells over-expressing BCL-xL or empty vector were exposed to a range of UV irradiation in the presence of Q-VD-OPH. MHM from these cells were subjected to carbonate extraction (Eskes et al., 2000), and presence of BAX in the sodium carbonate-resistant pellet fraction was assessed by Western-blot (Figure 6E). BAX was observed in the pellet fraction of HeLa cells exposed to both low and high UV intensity, correlating with

cytochrome *c* release. Interestingly, high UV intensity was able to trigger membrane insertion of BAX in the absence of MOMP in HeLa-BCL-xL. Together, these results indicate that BAX sequestered in MODE 2 is 6A7 negative and inserts into the mitochondrial membrane, consistent with the "embedded together" model of anti-apoptotic protein function (Leber et al., 2007).

MODE 2 sequestration promotes mitochondrial fragmentation and affects the kinetics of MOMP upon de-repression

Consistent with pervious reports (Sheridan et al., 2008), we observed that BAX translocation in the absence of MOMP in stressed HeLa-BCL-xL cells is accompanied by mitochondrial fragmentation (Figure 6A). Studies have suggested that BAX and BAK are important regulators of mitochondrial dynamics, promoting mitochondrial fusion presumably through interaction with mitofusin-2 (Brooks et al., 2007; Delivani et al., 2006; Hoppins et al., 2011; Karbowski et al., 2006). As we observed an effect of apoptotic stimulation on mitochondrial morphology only at later time-points when BAX accumulated on mitochondria, we hypothesized that MODE 2 and not MODE 1 sequestration influences mitochondrial dynamics. HeLa cells stably expressing Cerulean-OMM (Cerulean targeted to the outer mitochondria membrane by fusion to the C-terminal region of BCL-xL) and over-expressing BCL-xL were transfected with mCherry-tBID (Figure 7A). The connectivity of the mitochondrial network was assessed by FRAP (Fluorescence Recovery After Photobleaching) analysis of the Cerulean mitochondrial marker (Figure 7B). While low levels of mCherry-tBID expression did not affect mitochondrial morphology, higher levels induced pronounced fragmentation of the mitochondrial network. Accordingly, only high levels of tBID were able to induce BAK activation (Figure 5B). Similar results occurred when HeLa cells over-expressing BCL-xL were exposed to low versus high intensities of UV irradiation (Figure S5A). Thus, MODE 1 inhibition has marginal effect on mitochondrial morphology while MODE 2 sequestration promotes mitochondrial fragmentation, presumably by inhibition of mitochondrial fusion.

We next examined the consequences of the two sequestration modes on cell death upon de-repression. Based on the differential efficiency of the two modes, we reasoned that MOMP should occur with different kinetics upon de-repression of stressed cells in which one or the other mode of sequestration is predominant, provided that de-repressor concentrations are high enough to override both modes of inhibition. HeLa cells expressing Omi-mCherry and over-expressing BCL-xL were transfected with GFP-tBID and subsequently subjected to ABT-737 treatment 30 hr later (Figure 7C). Mean GFP intensity at the mitochondria was measured to determine the relative amount of tBID in each cell and MOMP was monitored by live cell imaging (Figures 7D). Counter-intuitively, we found that cells "primed for death" (Certo et al., 2006) with lower levels of tBID underwent MOMP upon ABT-737 treatment significantly faster than those with high tBID (Figures 7C and 7D). Interestingly, the onset of MOMP after de-repression did not appear to be strictly correlated with the amount of tBID but to rather follow two phases in agreement with a bi-modal inhibition model (Figure 7D). Below a threshold intensity value of 30000 (presumably corresponding to MODE 1 inhibition), cells underwent MOMP almost simultaneously with ABT-737 treatment, which suggests that under high de-repression conditions, MODE 1 directly proceeds to MOMP. Above that level, the time to onset of MOMP following ABT-737 treatment became proportional to the amount of tBID present and presumably to the concentration of effector proteins sequestered in MODE 2 (Figure 7D). Thus we speculate that this cell population displays a mix of MODE 1 and MODE 2 inhibition and becomes refractory to de-repression proportionally to the amount of BAX and BAK sequestered in MODE 2.

In a similar experiment, HeLa cells expressing Omi-mCherry and over-expressing BCL-xL or a vector control were treated with 5 and 40 mJ/cm^2 UV, conditions where we observed mainly MODE 1 and MODE 2 repression, respectively (Figures 6C and 6D). In the absence of ectopic BCL-xL both doses of UV triggered apoptosis, but not in the presence of BCL-xL (Figure S5B). After 30 h, the treated BCL-xL over-expressing cells were supplemented with ABT-737 and the kinetics of MOMP were assessed (Figure S5C). The onset of MOMP following treatment with ABT-737 was significantly faster in cells subjected to the lower dose of UV than those subjected to the higher dose. Consistent with previous work (Lopez et al., 2010), we found that knock-down of BIM, but not PUMA, significantly decreased UV induced cell death in HeLa cells (Figure S5D). Thus, like tBID in our previous experiment, BIM appears to induce MODE 2 sequestration in a stimulus intensity-dependent manner. Although no significant changes in BIM protein levels were detected in UV stimulated HeLa-BCL-xL cells, decreased levels of MCL-1 likely account for the pro-apoptotic activity of BIM in these cells (Figure S5E). We also verified that the protein levels of BAX, BAK, BCL-2 and BCL-xL were not affected by UV stimulation in HeLa cells (Figure S5E). Only PUMA levels were significantly higher in cells stimulated with 40 mJ/cm^2, and thus cannot account for the refractory kinetics of MOMP observed in these cells.

As the conditions under which we engage MODE 2 (high tBID, high UV) promote mitochondrial fragmentation (see above), fragmentation itself could be responsible for the cells being relatively refractory to de-repression by ABT-737. To test this, we inhibited mitochondrial fusion in HeLa cells by addition of the uncoupler FCCP, and subjected them to UV irradiation to trigger MOMP. Although mitochondria fragmented in presence of FCCP, we observed no effect on the rates of MOMP (Figure S5F). HeLa cells expressing Omi-mCherry and over-expressing BCL-xL were transfected with GFP-tBID and the status of the mitochondria (tubular versus fragmented) was examined, after which ABT-737 was added and MOMP time-course assessed. Consistently, cells expressing lower levels of tBID and displaying tubular mitochondria (MODE 1) underwent MOMP faster than those expressing higher levels of tBID and displaying fragmented mitochondria (MODE 2) (Figure 7E). Thus, the effects of MODE 1 versus MODE 2 sequestration can produce an *apparent* relationship between mitochondrial dynamics (fragmented versus fused) and MOMP. Together these results suggest that cells “primed for death” can be divided into two groups based on the prevalence of MODE 1 or MODE 2 sequestration and that these two populations undergo MOMP with different kinetics upon de-repression.

Discussion

Functional interactions between BCL-2 family proteins control the mitochondrial pathway of apoptosis. How these interactions dictate MOMP occurrence remains controversial. To establish a unifying model for the interaction hierarchy for anti-apoptotic BCL-2 proteins inhibition of MOMP, we designed chimeric direct activators (tBID$^{BAX\text{-}BH3}$ and tBID$^{BAK\text{-}BH3}$) that can activate both BAX and BAK, but are not universally sequestered by anti-apoptotic proteins like “wild type” direct activators (e.g. BID, BIM) (Figure 1, 2A, 2B and 2C). This enabled us to define two modes by which anti-apoptotic BCL-2 proteins can inhibit MOMP: by sequestering BH3-only direct activator proteins (MODE 1) or the active effectors BAX and BAK (MODE 2) (Figure 2D, 2E and 2F). While both are competent to inhibit MOMP, MODE 1 sequestration is less efficient than MODE 2, and more readily de-repressed to cause MOMP (Figure 4). As biochemical studies looking directly at the formation of MODE 2 complexes are often biased by the use of detergents known to affect BAX and BAK conformation (Hsu and Youle, 1997) (see also Figure 3A), we developed an assay based on limited calpain proteolysis to monitor the status of native BAK: inactive, active or sequestered by anti-apoptotic BCL-2 proteins (Figure 3 and S2). Similarly, BAX translocation and insertion into membranes was used as readout for BAX activation

irrespective of MOMP (Figure 6). These tools allowed us to dissect the mechanisms underling BCL-2 proteins interactions.

Since anti-apoptotic BCL-2 family members can inhibit both direct activator and effector proteins, what are the dynamics of MOMP inhibition upon apoptosis induction? Our data support a model in which BAX (cytosolic) and BAK (mitochondrial) reside in an inactive/dormant state in healthy cells not "kept in check" by anti-apoptotic proteins (Figures 5 and 6, see also Figure S7). Upon apoptotic stimulation, direct activators are produced and sequestered by anti-apoptotic proteins (MODE 1). Despite their seemingly high affinity, these interactions are reversible, allowing free direct-activator to persist even when anti-apoptotic proteins are found in excess (see Figure S6). At low stress levels, the concentration of unbound direct-activator is negligible and insufficient to activate BAX or BAK. Under high stress conditions however, the amount of direct-activator in the cell increases and with it the unbound fraction, allowing for BAX and BAK activation (Figure S6). Since MODE 2 repression is more efficient than MODE1 (Figure 4), the active effectors are in turn sequestered by anti-apoptotic proteins to form MODE 2 complexes (Figure 5 and 6, see also model in Figure S7).

This dual engagement model supports extremely rapid mitochondrial translocation of BAX upon apoptosis induction in cellular scenarios where anti-apoptotic levels are low (Figure 6A and Movie S1) whereas anti-apoptotic over-expression enables a delayed and gradual translocation (Figures 6B and Movie S2). Similarly, BAK activation (as seen in its sequestered form) is greatly reduced in cells over-expressing BCL-xL (Figure 5C). This phenomenon suggests that BAX and BAK activation is the result of two reactions: direct activators first engage and activate a fraction of the effector proteins, which then participate in activating the remaining pool of inactive BAX and BAK in a feed-forward manner (Gavathiotis et al., 2010). Over-expression of BCL-xL greatly reduces the availability of direct activator in these cells and also blocks any newly generated molecule of active BAX or BAK, inhibiting the feed-forward activation and considerably slows the rate of effector activation. Additionally, we can speculate that the inhibition of this auto-activation process participates in the relative higher efficiency of MODE 2 sequestration, which blocks a process of rapid auto-amplification, compared to MODE 1 that requires efficient sequestration of all of the direct activator BH3-only protein to remain an effective inhibitory mechanism.

Our model is consistent with the "embedded together" model (Leber et al., 2007; Leber et al., 2010) which proposes that active BAX and BAK, bound to anti-apoptotic BCL-2 proteins, are embedded in the mitochondrial outer membrane, which prevents pore formation resulting in MOMP. We found that in MODE 2 sequestration, BAX is resistant to extraction by sodium carbonate, indicating insertion of BAX into the membrane in its inhibited form. Interactions between the anti-apoptotic and effector proteins in this setting that may extend beyond the BH3-hydrophic groove interface (Ding et al., 2010; Ku et al., 2011) likely account for the increased efficiency we observe for MODE 2 sequestration, and for its relative resistance to de-repression. Accordingly, we found that BAX 6A7 epitope is not accessible in MODE 2 complexes, suggesting that the interaction with anti-apoptotic BCL-2 proteins extends to (or, at least, affects) the N-terminal region of BAX.

It has been proposed that BAX is sustained in its cytosolic inactive conformation in healthy cells though constant retro-translocation from the mitochondria, mediated by transient interaction with BCL-xL (Edlich et al., 2011), yet we observed mitochondrial BAX accumulation without MOMP in UV irradiated BCL-xL over-expressing HeLa cells (Figure 6). We can envision two scenarios in which BAX and BCL-xL interact. In healthy cells, inactive cytosolic BAX randomly collides with the mitochondria, in which case no

membrane integration occurs and binding to BCL-xL results in retro-translocation. In stressed cells, transient interaction with direct activators induces extensive conformational changes of BAX resulting in the formation of a more stable, membrane embedded complex with BCL-xL. In the model we propose here, only the later represents “MODE 2” sequestration.

The BCL-2 family is linked to mitochondrial physiology by modulating mitochondrial dynamics. In dying cells, BAX activation and MOMP coincide with mitochondrial fragmentation (Frank et al., 2001; Karbowski et al., 2002). Conversely, BAX and BAK positively regulate mitochondrial fusion in healthy cells (Karbowski et al., 2006). Interestingly, MODE 1 sequestration had little effect on mitochondrial morphology, whereas the activation of BAX and BAK and their subsequent sequestration by anti-apoptotic proteins (MODE 2) induced fragmentation of the mitochondrial network (Figures 7A, 7B and Figure S5). These results agree with work showing that BAX and BAK can promote mitochondrial fission without inducing MOMP when inhibited by anti-apoptotic proteins (Sheridan et al., 2008) and support the idea that the inactive effectors positively regulate mitochondrial fusion. In stimulated cells, active BAX and BAK (free or antagonized by anti-apoptotic BCL-2 proteins) no longer promote fusion, resulting in the collapse of the mitochondrial network (Figure S7). This view is supported by a recent study showing that the soluble form of BAX positively regulates mitochondrial fusion through binding to MFN2 (Hoppins et al., 2011). Hence, in primed cells, the two modes of inhibition have distinct physiological consequences.

This bi-modal inhibition model helps to explain the paradoxical finding that cells primed by high apoptotic stimulation can die less efficiently than cells exposed to low stimulation in response to ABT-737 treatment (Figures 7C, 7D, and Figure S5C). Since MODE 1 complexes are less stable than MODE 2 (Figure 4), cells subjected to low stress and, as a consequence, displaying predominantly MODE 1 complexes respond more readily to high doses of de-repression. As the intensity of the stimulation increases, cells shift from a MODE 1 to a predominantly MODE 2 repression, resulting in a significant delay in MOMP in response to ABT-737 treatment (Figure S7).

Our “unified” model of anti-apoptotic BCL-2 protein function is consistent with previous models (as discussed), but incorporates the differential efficiencies of each mode of action into the consequences for the cell fate. In doing so, our model helps to explain seemingly paradoxical phenomena in BCL-2 family function and provides a framework for predicting cellular behavior in “life or death” decision-making. Our current work may reenergize efforts to target the mitochondrial pathway of apoptosis in pathophysiology with improved inhibitors of MODE 2 sequestration. We have begun to incorporate the functions of the BCL-2 proteins in mitochondrial dynamics, but additional work on the functions of these proteins in the regulation of autophagy, calcium homeostasis, and metabolism (Chipuk et al., 2010) will be required to attain a more complete understanding of the complex behavior of this important protein family.

Experimental Procedures

In vitro cytochrome c release assay

Mitochondria-enriched heavy membrane (MHM) fractions were purified from mouse liver using dounce homogenization and differential centrifugation in mitochondrial isolation buffer (MIB: 200 mM mannitol, 68 mM sucrose, 10 mM HEPES-KOH pH 7.4, 10 mM KCl, 1 mM EDTA, protease inhibitors (Complete, Roche)). For cytochrome *c* release assays, MHM were incubated with the indicated IVTT and/or recombinant proteins in MIB supplemented to 110 mM KCl for 60 min at 37°C. Reactions were then fractionated into

supernatant and pellet by centrifugation at 5,500 g for 5 min and analyzed by SDS/PAGE and Western blot with anti-cytochrome c.

BAK limited proteolysis by calpain

For *in vitro* assays, MHM fractions extracted from mouse liver were washed twice with calpain assay buffer (CAB: 200 mM mannitol, 68 mM sucrose, 10 mM HEPES-KOH pH 7.4, 10 mM KCl) and incubated with the indicated IVTT and/or recombinant proteins. Reactions were then incubated with 20 nM calpain in CAB plus 0.5 mM $CaCl_2$ for 30 min at room temperature and analyzed by SDS/PAGE and Western blot with anti-BAK(G23) antibody. For BAK limited proteolysis in HeLa cells, 10^5 cells were washed twice in cold CAB and incubated for 10 min on ice in CAB plus 200 μg/mL digitonin. Cells were washed twice in cold CAB then incubated with 20 nM calpain in CAB plus 0.5 mM $CaCl_2$ for 30 min at room temperature. Cells were then lysed in cell lysis buffer (50mM Tris-Cl, pH 7.4, 150mM NaCl, protease inhibitors (Complete, Roche) plus 2% CHAPS) and analyzed by SDS/PAGE and Western blot with anti-BAK(G23) antibody.

Sodium carbonate extraction

Alkali extraction of mitochondrial proteins was performed as previously described (Eskes et al., 2000). Briefly, HeLa cells were resuspended in MIB and lysed by a series of passages through a 25G1 needle. MHM fractions were purified by differential centrifugation, resuspended in 0.1 M Na_2CO_3 (pH 11.5) and incubated for 20 min on ice. The membranes were then pelleted by centrifugation (100,000 g for 30 min at 4°C) and analyzed by SDS/PAGE and Western blot with anti-BAX or anti-BAK antibodies.

Supplementary Material

Refer to Web version on PubMed Central for supplementary material.

Acknowledgments

We thank Abbott Laboratories for providing ABT-737. We also thank Samuel Connell (Intelligent Imaging Innovations, Inc) for invaluable advice and discussion and Richard Cross, Greig Lennon and Stephanie Morgan (St. Jude Flow Cytometry facility) for cell sorting. This work was supported by NIH grants AI40646, GM52735, and GM096208 (DRG) and the American Lebanese Syrian Associated Charities.

Bibliography

Adler J, Parmryd I. Quantifying colocalization by correlation: the Pearson correlation coefficient is superior to the Mander's overlap coefficient. Cytometry A. 2010; 77:733–742. [PubMed: 20653013]

Brooks C, Wei Q, Feng L, Dong G, Tao Y, Mei L, Xie ZJ, Dong Z. Bak regulates mitochondrial morphology and pathology during apoptosis by interacting with mitofusins. Proc Natl Acad Sci USA. 2007; 104:11649–11654. [PubMed: 17606912]

Certo M, Del Gaizo Moore V, Nishino M, Wei G, Korsmeyer S, Armstrong SA, Letai A. Mitochondria primed by death signals determine cellular addiction to antiapoptotic BCL-2 family members. Cancer Cell. 2006; 9:351–365. [PubMed: 16697956]

Chen L, Willis SN, Wei A, Smith BJ, Fletcher JI, Hinds MG, Colman PM, Day CL, Adams JM, Huang DCS. Differential targeting of prosurvival Bcl-2 proteins by their BH3-only ligands allows complementary apoptotic function. Molecular Cell. 2005; 17:393–403. [PubMed: 15694340]

Chipuk JE, Moldoveanu T, Llambi F, Parsons MJ, Green DR. The BCL-2 family reunion. Molecular Cell. 2010; 37:299–310. [PubMed: 20159550]

Delivani P, Adrain C, Taylor RC, Duriez PJ, Martin SJ. Role for CED-9 and Egl-1 as regulators of mitochondrial fission and fusion dynamics. Molecular Cell. 2006; 21:761–773. [PubMed: 16543146]

Dewson G, Kratina T, Sim HW, Puthalakath H, Adams JM, Colman PM, Kluck RM. To trigger apoptosis, Bak exposes its BH3 domain and homodimerizes via BH3:groove interactions. Molecular Cell. 2008; 30:369–380. [PubMed: 18471982]

Ding J, Zhang Z, Roberts GJ, Falcone M, Miao Y, Shao Y, Zhang XC, Andrews DW, Lin J. BCL-2 and bax interact via the BH1-3 groove:BH3 motif interface and a novel interface involving the BH4 motif. J Biol Chem. 2010; 285:28749–28763. [PubMed: 20584903]

Edlich F, Banerjee S, Suzuki M, Cleland MM, Arnoult D, Wang C, Neutzner A, Tjandra N, Youle RJ. Bcl-x(L) retrotranslocates Bax from the mitochondria into the cytosol. Cell. 2011; 145:104–116. [PubMed: 21458670]

Eskes R, Desagher S, Antonsson B, Martinou JC. Bid induces the oligomerization and insertion of Bax into the outer mitochondrial membrane. Mol Cell Biol. 2000; 20:929–935. [PubMed: 10629050]

Frank S, Gaume B, Bergmann-Leitner ES, Leitner WW, Robert EG, Catez F, Smith CL, Youle RJ. The role of dynamin-related protein 1, a mediator of mitochondrial fission, in apoptosis. Dev Cell. 2001; 1:515–525. [PubMed: 11703942]

Friedrich P, Bozóky Z. Digestive versus regulatory proteases: on calpain action in vivo. Biol Chem. 2005; 386:609–612. [PubMed: 16207081]

Gavathiotis E, Reyna DE, Davis ML, Bird GH, Walensky LD. BH3-triggered structural reorganization drives the activation of proapoptotic BAX. Molecular Cell. 2010; 40:481–492. [PubMed: 21070973]

Hoppins S, Edlich F, Cleland MM, Banerjee S, McCaffery JM, Youle RJ, Nunnari J. The Soluble Form of Bax Regulates Mitochondrial Fusion via MFN2 Homotypic Complexes. Molecular Cell. 2011; 41:150–160. [PubMed: 21255726]

Hsu YT, Wolter KG, Youle RJ. Cytosol-to-membrane redistribution of Bax and Bcl-X(L) during apoptosis. Proc Natl Acad Sci USA. 1997; 94:3668–3672. [PubMed: 9108035]

Hsu YT, Youle RJ. Nonionic detergents induce dimerization among members of the Bcl-2 family. J Biol Chem. 1997; 272:13829–13834. [PubMed: 9153240]

Karbowski M, Lee YJ, Gaume B, Jeong SY, Frank S, Nechushtan A, Santel A, Fuller M, Smith CL, Youle RJ. Spatial and temporal association of Bax with mitochondrial fission sites, Drp1, and Mfn2 during apoptosis. J Cell Biol. 2002; 159:931–938. [PubMed: 12499352]

Karbowski M, Norris KL, Cleland MM, Jeong SY, Youle RJ. Role of Bax and Bak in mitochondrial morphogenesis. Nature. 2006; 443:658–662. [PubMed: 17035996]

Kim H, Rafiuddin-Shah M, Tu HC, Jeffers JR, Zambetti GP, Hsieh JJD, Cheng EHY. Hierarchical regulation of mitochondrion-dependent apoptosis by BCL-2 subfamilies. Nat Cell Biol. 2006; 8:1348–1358. [PubMed: 17115033]

Kim H, Tu HC, Ren D, Takeuchi O, Jeffers JR, Zambetti GP, Hsieh JJD, Cheng EHY. Stepwise activation of BAX and BAK by tBID, BIM, and PUMA initiates mitochondrial apoptosis. Molecular Cell. 2009; 36:487–499. [PubMed: 19917256]

Ku B, Liang C, Jung JU, Oh BH. Evidence that inhibition of BAX activation by BCL-2 involves its tight and preferential interaction with the BH3 domain of BAX. Cell Res. 2011; 21:627–641. [PubMed: 21060336]

Kuwana T, Bouchier-Hayes L, Chipuk JE, Bonzon C, Sullivan BA, Green DR, Newmeyer DD. BH3 domains of BH3-only proteins differentially regulate Bax-mediated mitochondrial membrane permeabilization both directly and indirectly. Molecular Cell. 2005; 17:525–535. [PubMed: 15721256]

Kuwana T, Mackey MR, Perkins G, Ellisman MH, Latterich M, Schneiter R, Green DR, Newmeyer DD. Bid, Bax, and lipids cooperate to form supramolecular openings in the outer mitochondrial membrane. Cell. 2002; 111:331–342. [PubMed: 12419244]

Kvansakul M, Yang H, Fairlie WD, Czabotar PE, Fischer SF, Perugini MA, Huang DCS, Colman PM. Vaccinia virus anti-apoptotic F1L is a novel Bcl-2-like domain-swapped dimer that binds a highly selective subset of BH3-containing death ligands. Cell Death Differ. 2008; 15:1564. [PubMed: 18551131]

Leber B, Lin J, Andrews DW. Embedded together: the life and death consequences of interaction of the Bcl-2 family with membranes. Apoptosis. 2007; 12:897–911. [PubMed: 17453159]

Leber B, Lin J, Andrews DW. Still embedded together binding to membranes regulates Bcl-2 protein interactions. Oncogene. 2010; 29:5221–5230. [PubMed: 20639903]

Letai A, Bassik MC, Walensky LD, Sorcinelli MD, Weiler S, Korsmeyer SJ. Distinct BH3 domains either sensitize or activate mitochondrial apoptosis, serving as prototype cancer therapeutics. Cancer Cell. 2002; 2:183–192. [PubMed: 12242151]

Llambi F, Green DR. Apoptosis and oncogenesis: give and take in the BCL-2 family. Curr Opin Genet Dev. 2011; 21:12–20. [PubMed: 21236661]

Lopez H, Zhang L, George NM, Liu X, Pang X, Evans JJD, Targy NM, Luo X. Perturbation of the Bcl-2 network and an induced Noxa/Bcl-xL interaction trigger mitochondrial dysfunction after DNA damage. J Biol Chem. 2010; 285:15016–15026. [PubMed: 20223826]

Martinou JC, Youle RJ. Mitochondria in apoptosis: bcl-2 family members and mitochondrial dynamics. Dev Cell. 2011; 21:92–101. [PubMed: 21763611]

Mérino D, Giam M, Hughes PD, Siggs OM, Heger K, O'Reilly LA, Adams JM, Strasser A, Lee EF, Fairlie WD, Bouillet P. The role of BH3-only protein Bim extends beyond inhibiting Bcl-2-like prosurvival proteins. J Cell Biol. 2009; 186:355–362. [PubMed: 19651893]

Oltersdorf T, Elmore SW, Shoemaker AR, Armstrong RC, Augeri DJ, Belli BA, Bruncko M, Deckwerth TL, Dinges J, Hajduk PJ, et al. An inhibitor of Bcl-2 family proteins induces regression of solid tumours. Nature. 2005; 435:677–681. [PubMed: 15902208]

Petros AM, Olejniczak ET, Fesik SW. Structural biology of the Bcl-2 family of proteins. Biochim Biophys Acta. 2004; 1644:83–94. [PubMed: 14996493]

Sattler M, Liang H, Nettesheim D, Meadows RP, Harlan JE, Eberstadt M, Yoon HS, Shuker SB, Chang BS, Minn AJ, et al. Structure of Bcl-xL-Bak peptide complex: recognition between regulators of apoptosis. Science. 1997; 275:983–986. [PubMed: 9020082]

Sheridan C, Delivani P, Cullen SP, Martin SJ. Bax- or Bak-induced mitochondrial fission can be uncoupled from cytochrome C release. Molecular Cell. 2008; 31:570–585. [PubMed: 18722181]

Uren RT, Dewson G, Chen L, Coyne SC, Huang DCS, Adams JM, Kluck RM. Mitochondrial permeabilization relies on BH3 ligands engaging multiple prosurvival Bcl-2 relatives, not Bak. J Cell Biol. 2007; 177:277–287. [PubMed: 17452531]

Wei MC, Lindsten T, Mootha VK, Weiler S, Gross A, Ashiya M, Thompson CB, Korsmeyer SJ. tBID, a membrane-targeted death ligand, oligomerizes BAK to release cytochrome c. Genes Dev. 2000; 14:2060–2071. [PubMed: 10950869]

Willis SN, Chen L, Dewson G, Wei A, Naik E, Fletcher JI, Adams JM, Huang DCS. Proapoptotic Bak is sequestered by Mcl-1 and Bcl-xL, but not Bcl-2, until displaced by BH3-only proteins. Genes Dev. 2005; 19:1294–1305. [PubMed: 15901672]

Willis SN, Fletcher JI, Kaufmann T, van Delft MF, Chen L, Czabotar PE, Ierino H, Lee EF, Fairlie WD, Bouillet P, et al. Apoptosis initiated when BH3 ligands engage multiple Bcl-2 homologs, not Bax or Bak. Science. 2007; 315:856–859. [PubMed: 17289999]

Zhai D, Jin C, Huang Z, Satterthwait A, Reed J. Differential regulation of Bax and Bak by anti-apoptotic Bcl-2-family proteins, Bcl-B and Mcl-1. J Biol Chem. 2008; 283:9580–9586. [PubMed: 18178565]

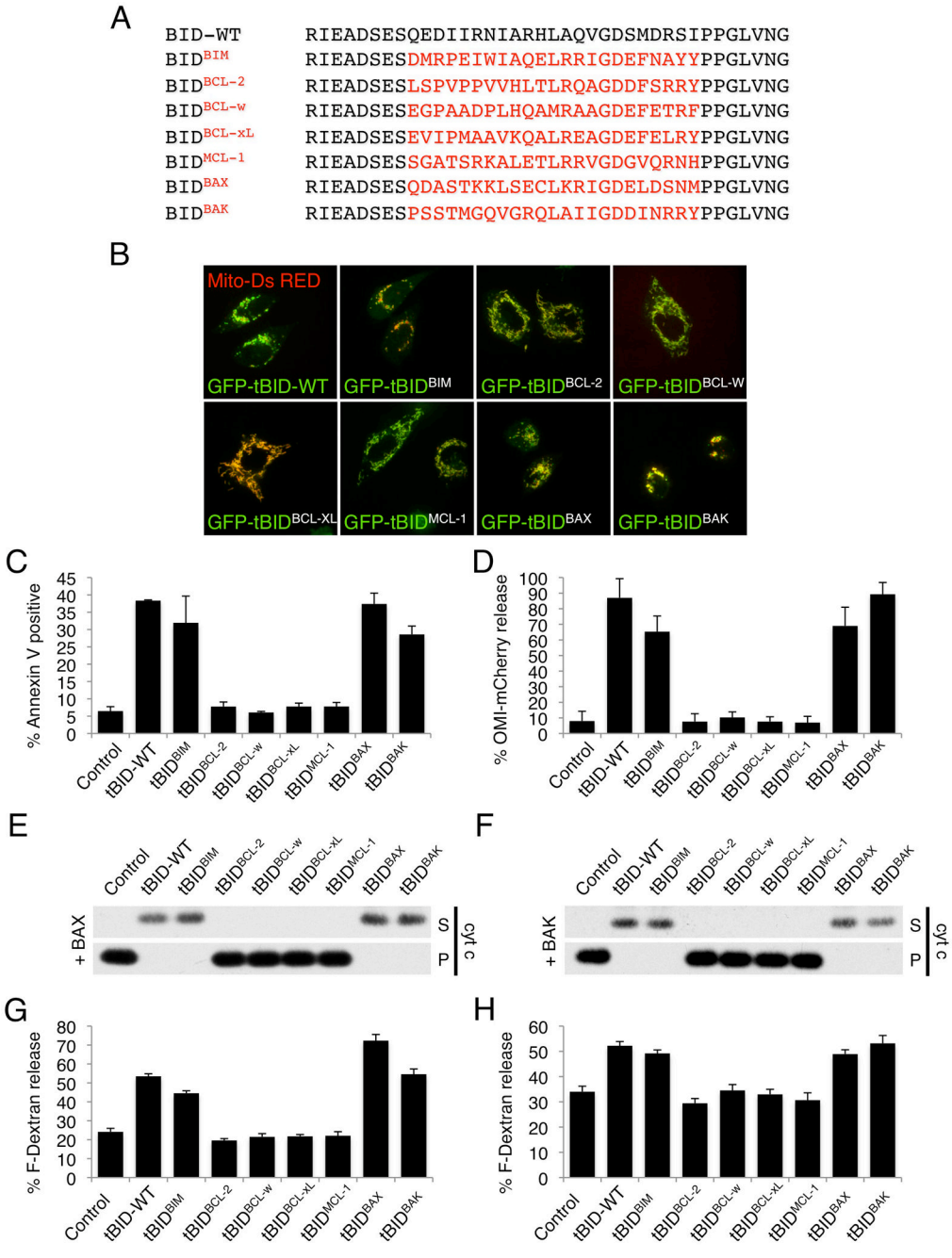

Figure 1. tBID$^{BAX\text{-}BH3}$ and tBID$^{BAK\text{-}BH3}$ directly activate BAX and BAK

(A) Sequence alignment of the BH3 domains used to generate the tBID^{BH3} chimeras. **(B)** HeLa cells were co-transfected with mitochondrial matrix targeted dsRed (mito-dsRed) and the indicated GFP-tBID^{BH3} chimera in presence of Q-VD-OPH (20 μM) and imaged after 24 hr by live-cell confocal microscopy. Representative micrographs are shown. **(C)** HeLa cells were transfected with the indicated tBID^{BH3} chimeras and apoptotic cell death was quantified after 24 hr by Annexin V staining and flow cytometry analysis. **(D)** HeLa cells stably expressing Omi-mCherry were transfected with tBID^{BH3} chimeras and scored for mitochondrial versus cytosolic Omi-mCherry localization after 24 hr. **(E)** Mitochondria-enriched heavy membrane (MHM) fractions extracted from *bak*$^{-/-}$ C57BL/6 mouse liver

were incubated with 10 nM purified recombinant BAX and IVTT (in vitro transcription and translation) from wheat germ extract expressing the indicated $tBID^{BH3}$ chimera for 1 hr at 37°C. Supernatant (S) and pellet (P) fractions were then separated by centrifugation and cytochrome *c* release was monitored by Western blot. **(F)** MHM extracted from WT C57BL/6 mouse liver were treated as in (E) in the absence of recombinant BAX. **(G)** Large Unilamelar Vesicles (LUV) containing Fuorescein-Dextran were incubated with IVTT of the indicated $tBID^{BH3}$ chimera in presence of 120 nM purified recombinant BAX. LUV permeabilization is shown as % release of Fluorescein-Dextran. **(H)** LUV were incubated as in (G) in presence of 500 nM purified recombinant BAK-ΔC (lacking the C-terminus). Error bars represent standard deviation from triplicate data.
(See also Figure S1)

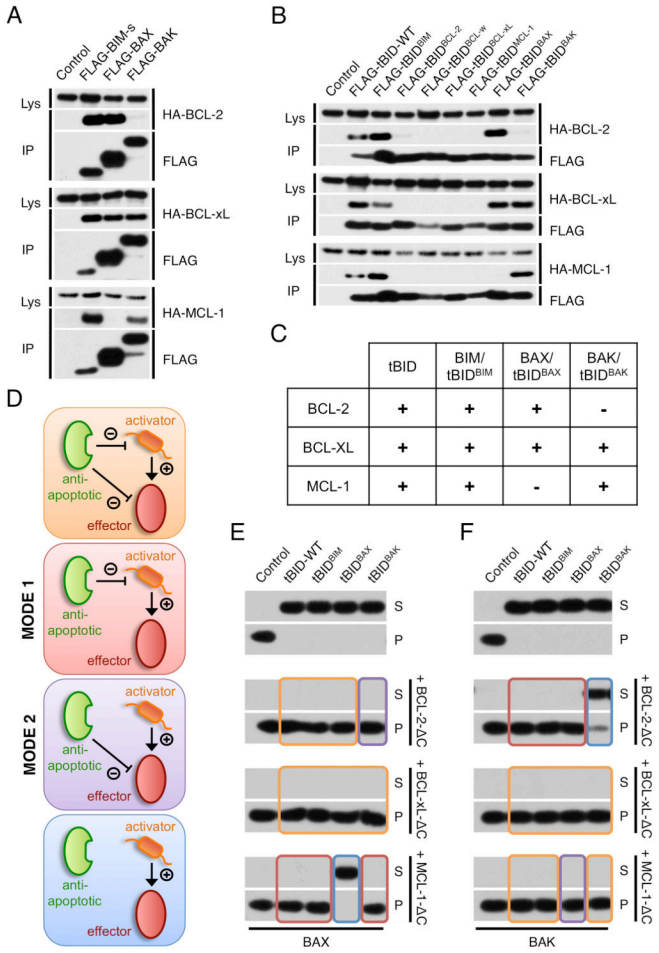

Figure 2. Anti-apoptotic BCL-2 proteins inhibit MOMP by sequestering BH3-only and effector proteins

(A/B) HEK-293T cells were transiently transfected with plasmid encoding HA-tagged BCL-2, BCL-xL and MCL-1 together with FLAG-tagged BIM-s, BAX, BAK (A) or the indicated FLAG-tBID^{BH3} chimera (B). Cells were lysed in 0.5% NP40 and protein complexes were immunoprecipitated with an anti-FLAG antibody. Protein interactions were analyzed by Western blot using anti-HA and anti-FLAG antibodies (Lys: total cell lysate, IP: immunoprecipitation). **(C)** Interaction profile of tBID^{BH3} chimeras and effector proteins with anti-apoptotic BCL-2 proteins as experimentally determined by immunoprecipitation in (A) and (B). **(D)** Schematic representation of possible scenarios for MOMP inhibition by anti-apoptotic BCL-2 proteins. **(E)** MHM fractions extracted from *bak*$^{-/-}$ C57BL/6 mouse liver were incubated for 1 hr at 37°C with IVTT of the indicated tBID^{BH3} chimera in presence of 10 nM purified recombinant BAX and 1 μM purified recombinant BCL-2-ΔC, BCL-xL-ΔC or MCL-1-ΔC. Supernatant (S) and pellet (P) fractions were then separated by centrifugation and cytochrome *c* release was monitored by Western blot. The boxes' colors correspond to the individual scenarios predicted in (D). **(F)** MHM extracted from WT C57BL/6 mouse liver were treated as in (D) in the absence of recombinant BAX.

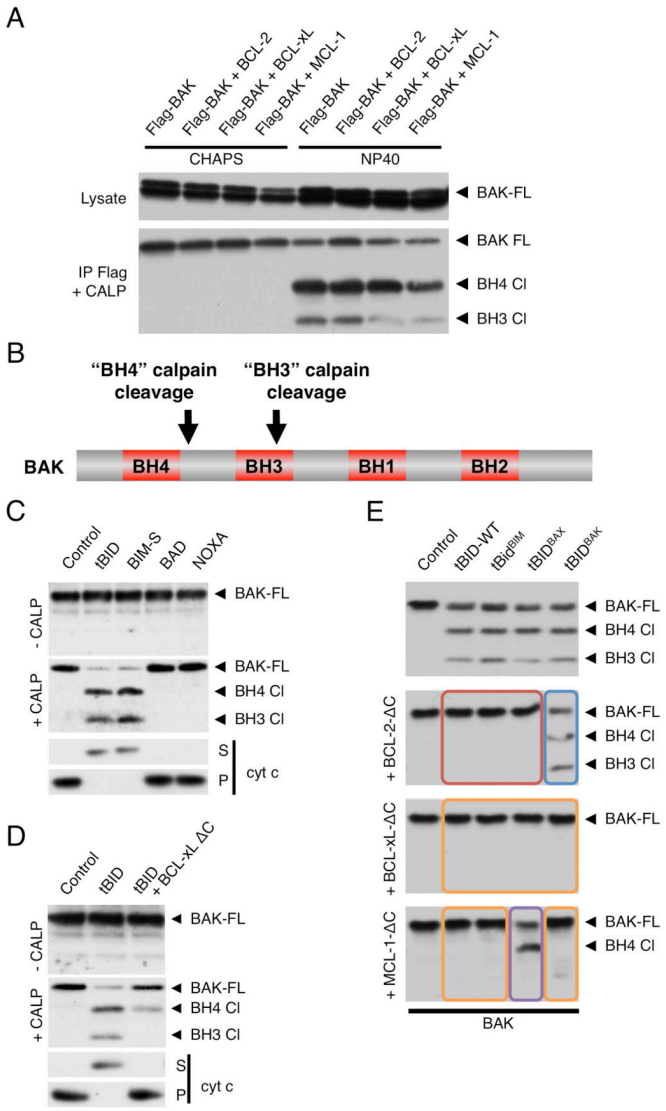

Figure 3. BAK conformational change upon activation is detected by limited calpain digestion

(A) HEK-293T cells stably expressing FLAG-BAK were transiently transfected with plasmids encoding HA-BCL-2, HA-BCL-xL, HA-MCL-1 or empty vector. FLAG-BAK was immunoprecipitated from cell lysates with anti-FLAG-agarose in 2% CHAPS or 0.5% NP40 as indicated and incubated with calpain (20 nM) in presence of $CaCl_2$ (0.5 mM) for 30 min at room temperature. BAK cleavage was monitored by Western blot using anti-BAK-G23 antibody. Full length BAK (BAK FL) and two cleavage fragments (BH4 Cl and BH3 Cl) are indicated with arrows **(B)** Schematic representation of the position of the two calpain cleavage sites in active BAK. **(C)** MHM fractions extracted from C57BL/6 mouse liver were incubated for 1 hr at 37°C with IVTT from wheat germ extract expressing tBID, BIM-s, BAD or NOXA and left untreated (upper panel) or incubated with calpain (20 nM) in presence of $CaCl_2$ (0.5 mM) for 30 min at room temperature (middle panel). BAK cleavage was monitored by Western blot using anti-BAK-G23 antibody. Supernatants (S) and mitochondrial pellets (P) were also analyzed for cytochrome *c* by Western blot (lower panel). **(D)** MHM fractions from C57BL/6 mouse liver were incubated with IVTT of tBID in the presence or absence of 50 nM purified recombinant BCL-xL-ΔC (lacking the C-terminus) and treated as in (C) for calpain proteolysis (upper panel) or monitored for

cytochrome *c* release (lower panel). **(E)** MHM fractions extracted from C57BL/6 mouse liver were incubated with IVTT of the indicated $tBID^{BH3}$ chimeras in presence of 1 μM purified recombinant BCL-2-ΔC, BCL-xL-ΔC or MCL-1-ΔC and treated as in (C) for calpain proteolysis. The boxes' colors correspond to the scenarios predicted in Figure 2D. (See also Figure S2)

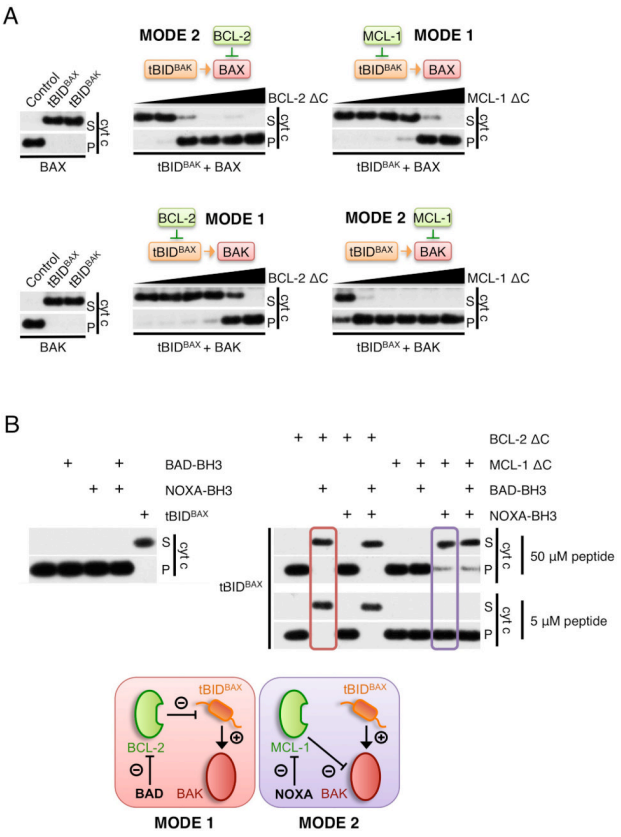

Figure 4. Inhibition of MOMP is less efficient in MODE 1 than in MODE 2

(A) MHM fractions from *bak*$^{-/-}$ (upper panels) or wild type C57BL/6 mouse liver (lower panels) were incubated with IVTT from wheat germ extract expressing the indicated tBID^{BH3} chimeras, 10 nM recombinant BAX (upper panels only) and increasing concentrations of recombinant BCL-2-ΔC or MCL-1-ΔC (0, 4, 12, 37,111, 333 and 1000 nM) for 1 hr at 37°C. Supernatant (S) and pellet (P) fractions were then separated by centrifugation and cytochrome *c* release was monitored by Western blot. **(B)** MHM fractions extracted from wild type C57BL/6 mouse liver were left untreated (right panel) or incubated with 1 μM recombinant BCL-2-ΔC or MCL-1-ΔC (left panel). When indicated, reactions were supplemented with IVTT of tBID$^{BAX\text{-}BH3}$ for 1h at 37°C. Reactions were then de-repressed with addition of BAD-BH3 or NOXA-BH3 peptide (5 or 50 μM) for 1 hr at 37°C and monitored for cytochrome *c* release as in (A). Lower panel shows a schematic representation of MODE 1 (red) versus MODE 2 de-repression (purple) used in this assay.

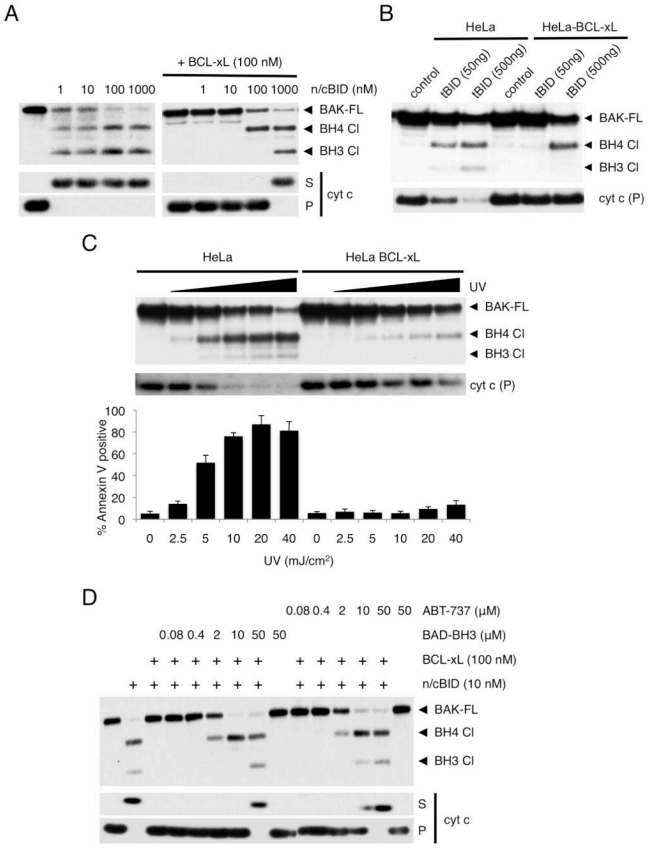

Figure 5. BCL-xL blocks MOMP sequentially through MODE 1 and MODE 2

(A) MHM fractions extracted from C57BL/6 mouse liver were incubated for 1 hr at 37°C with 100 nM full length recombinant BCL-xL and the indicated concentrations of cleaved recombinant BID (n/cBID). MHM were then incubated with calpain (20 nM) in presence of $CaCl_2$ (0.5 mM) for 1hr at room temperature. BAK cleavage was monitored by Western blot using anti-BAK-G23 antibody. Full-length BAK (BAK FL) and two cleavage fragments (BH4 Cl and BH3 Cl) are indicated with arrows. Supernatants (S) and mitochondrial pellets (P) were also analyzed for cytochrome *c* by Western blot. **(B)** HeLa cells stably over-expressing BCL-xL or an empty vector were transiently transfected with the indicated amount of tBID for 24 hr in presence of Q-VD-OPH (20 μM), permeabilized with digitonin (200 μg/ml) and incubated with calpain (20 nM) in presence of $CaCl_2$ (0.5 mM) for 30 min at room temperature. BAK cleavage was monitored by Western blot using anti-BAK-G23 antibody. Presence of cytochrome c was analyzed in pellet fractions (P) only as cytosolic components were lost during digitonin permeabilization. **(C)** HeLa cells stably over-expressing BCL-xL or an empty vector were exposed to increasing UV intensity (0, 2.5, 5, 10, 20 and 40 mJ/cm^2) in presence of Q-VD-OPH (20 μM). After 16 hr, cells were treated as in (B) for calpain proteolysis (upper panel) or monitored for cytochrome *c* release (middle panel). Apoptosis was assessed on intact cells by Annexin V staining and flow cytometry analysis (lower panel). Error bars represent standard deviation from triplicate data. **(D)** MHM fractions from C57BL/6 mouse liver were incubated for 1 hr at 37°C with full-length recombinant BCL-xL (100 nM) and n/cBID (10 nM). Reactions were then de-repressed with the indicated concentrations of BAD-BH3 peptide or ABT-737 for 1 hr at 37°C and treated as in (C) for calpain proteolysis (upper panel) or monitored for cytochrome *c* release (lower panel).

(See also Figure S3)

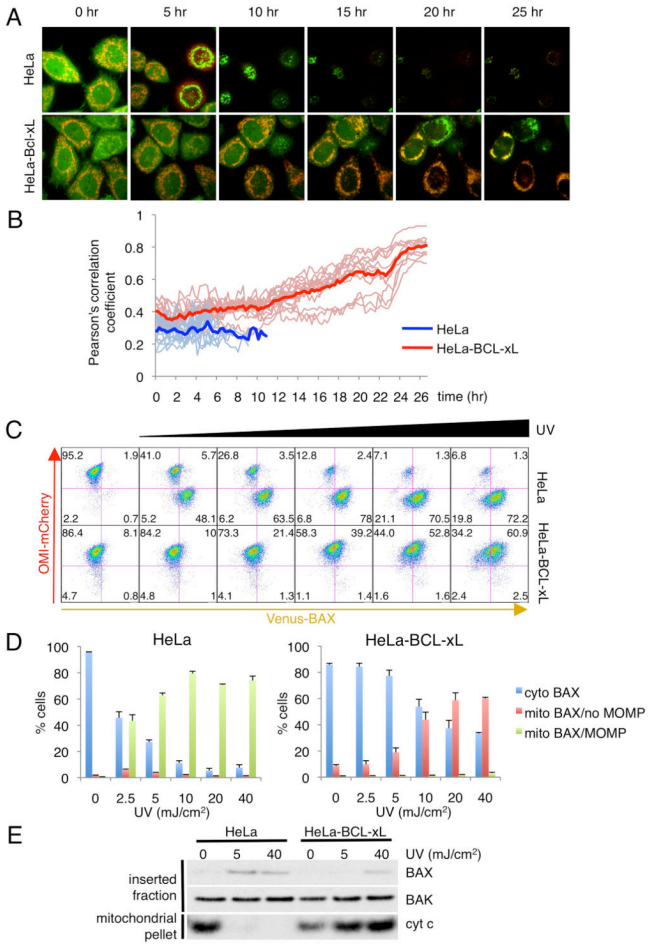

Figure 6. In the presence of BCL-xL, activated BAX translocates to the mitochondria without inducing MOMP

(A) HeLa cells stably expressing Venus-BAX and Omi-mCherry in the presence or absence of over-expressed BCL-xL, were exposed to 40 mJ/cm^2 UV plus Q-VD-OPH (20 nM) and imaged by live-cell confocal microscopy. Representative confocal micrographs are shown with the time of each frame relative to the time of stimulation. See also Movies S1 and S2. **(B)** To quantify BAX translocation in the absence of MOMP, co-localization between Venus-BAX and Omi-mCherry was measured by Pearson's correlation coefficient. Heavy lines represent the average of 15 individual cells (light lines) for each condition. Measurements were stopped when individual cells underwent MOMP. **(C)** HeLa cells stably expressing Venus-BAX and Omi-mCherry in the presence or absence of over-expressed BCL-xL, were exposed to 0, 2.5, 5, 10, 20 and 40 mJ/cm^2 UV in the presence of Q-VD-OPH (20 nM) for 30 hr. Cells were permeabilized with digitonin (200 μg/ml) and analyzed by flow cytometry. Representative dot plots are presented. **(D)** The percentage of cells representing mCherry^{high}/Venus^{low} (cyto BAX), mCherry^{high}/Venus^{high} (mito BAX/no MOMP) and mCherry^{low}/Venus^{high} (mito BAX/MOMP) groups is shown for HeLa cells (upper graph) and HeLa-BCL-xL cells (lower graph). Error bars represent standard deviation from triplicate data. **(E)** HeLa cells stably over-expressing BCL-xL or empty vector were exposed to 0, 5 or 40 mJ/cm^2 UV in presence of Q-VD-OPH (20 nM). After 30 hr, MHM fractions were extracted from the cells and analyzed by Western blot for cytochome c (mitochondrial pellet) or subjected to carbonate extraction and analyzed by Western blot for BAX and BAK (inserted fraction).

(See also Figure S4)

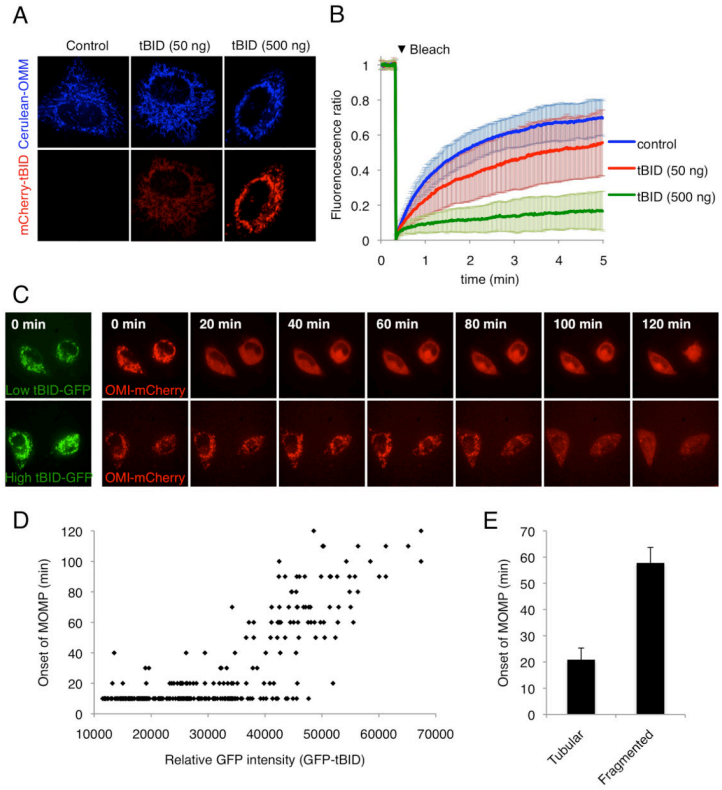

Figure 7. MODE 2 sequestration promotes mitochondrial fragmentation and affects the kinetics of MOMP upon de-repression

(A) HeLa cells stably expressing Cerulean-OMM (Cerulean protein targeted to the outer mitochondrial membrane by fusion to the C-terminal region of BCL-xL) and over-expressing BCL-xL were transfected with the indicated concentrations of mCherry-tBID plasmid for 30 hr. Representative confocal micrographs are shown. **(B)** Mitochondrial fragmentation was monitored by fluorescence recovery after photobleaching (FRAP) of the Cerulean-OMM. Each line of the graph is an average of 30 individual cells, error bars represent standard deviation. **(C)** HeLa cells expressing Omi-mCherry and over-expressing BCL-xL were transfected with GFP-tBID and treated after 30 hr with ABT-737 (20 μM) plus Q-VD-OPH (20 μM) and imaged every 10 min by live-cell confocal microscopy. Representative confocal micrographs are shown. The time of each frame relative to the time of ABT-737 addition is shown. **(D)** Cells were treated as in (C). GFP-tBID levels preceding ABT-737 treatment in individual cells were quantified by measuring the mean GFP signal intensity. Time of onset to MOMP was determined by monitoring Omi-mCherry release and was plotted as a function of GFP-tBID intensity. The graph represents the analysis of 300 individual cells from three independent experiments **(E)** Cells were treated as in (C); prior to ABT-737 treatment cells were scored for mitochondrial morphology (tubular vs. fragmented) and onset of MOMP was monitored as in (D). Error bars represent standard deviation from triplicate data.

(See also Figure S5)